Dalton Transactions

Cite this: *Dalton Trans.*, 2011, **40**, 12750

www.rsc.org/dalton

PAPER

Alkyltrioctylphosphonium chloride ionic liquids: synthesis and physicochemical properties

Gabriela Adamová,[a] Ramesh L. Gardas,[a,b] Luís Paulo N. Rebelo,[c] Allan J. Robertson[d] and Kenneth R. Seddon[a,c]

Received 25th February 2011, Accepted 4th July 2011
DOI: 10.1039/c1dt10332f

A series of alkyltrioctylphosphonium chloride ionic liquids, prepared from trioctylphosphine, and the respective 1-chloroalkane ($C_nH_{2n+1}Cl$), where n = 1, 2, 3, 4, 5, 6, 7, 8, 9, 10, 12 or 14, is presented. The cynosure of this work is the manner in which the variable chain length impacts the physical properties, such as melting points/glass transitions, thermal stability, density and viscosity. Experimental density and viscosity data were interpreted using QPSR correlations and group contribution methods. We present the first example of an empirical alternation effect for ionic liquids.

Introduction

Phosphonium salts represent an important sub-class of ionic liquids and became, over the past decade, an integral part of these industrially relevant solvents. An increasing trend in the number of publications enlarged their potential impact on industrial applications.[1] However, phosphonium-based ionic liquids were less systematically studied than their nitrogen-based counterparts (*e.g.* dialkylimidazolium, dialkylpyrollidinium, tetraalkylammonium, *etc.*).[2–4] In particular, it is somewhat surprising that there are no published data on ionic liquids of the type, $[P_{x\,x\,x\,n}]X$, where n is systematically varied, while keeping x constant. Restricting the phosphonium alkyl chains to being linear, with x and n having values between 1 and 20, the number of potential combinations is 400 ionic liquids for any given anion. Here, we present, for the first time, the systematic series of phosphonium chlorides (see Fig. 1), based on trioctylphosphine. Related studies of ionic liquids based on trihexylphosphine[5] and tributylphosphine[6] are in preparation.

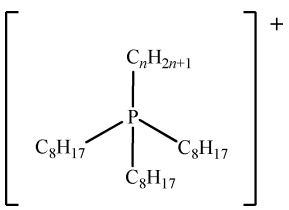

Fig. 1 The structure of the alkyltrioctylphosphonium cation, where n = 1, 2, 3, 4, 5, 6, 7, 8, 9, 10, 12 or 14.

The synthesis of phosphonium salts initially involves a nucleophilic substitution reaction between chloroalkane and a tertiary phosphine to produce a tetraalkylphosphonium halide which can be further converted, *via* anion exchange, into other ionic liquids.[7] The lack of available trialkylphosphines may have been one reason for the historically slow development of phosphonium ionic liquids. However, since the mid 80s a variety of trialkylphosphines, as well as a limited number of tetraalkylphosphonium halides have been commercially available from Cytec Industries, Inc.[8] As availability and cost of ionic liquids are paramount to any industrial applications, commercially available phosphonium ionic liquids can meet those demands and add many advantages in comparison with other families of ionic liquids, including for example higher thermal stability which allows them to be used in high temperature processes.[9] A high thermal stability was actually one of the reasons why Eastman Chemical Company (USA) employed $[P_{8\,8\,8\,18}]I$ as a Lewis basic ionic liquid in an isomerisation process of 3,4-epoxybut-1-ene to 2,5-dihydrofuran instead of its ammonium analogue, in 1996.[10] The process was successfully running for eight years with a capacity of 1400 metric tons per year.

Phosphonium salts are not necessarily liquid at room temperature, but by careful selection of the alkyl substituents, as well as an appropriate anion, there are many of them which fall within the broad definition of ionic liquids.[11] Traditionally, phosphonium-based halides represented by tetraethylphosphonium bromide or tetraphenylphosphonium chloride, have melting points above 270 °C[12] and therefore they are not usually considered, even in the broadest definition, as ionic liquids. Others, such as tetrabutylphosphonium chloride (m.p. 86 °C) or tetraoctylphosphonium bromide (m.p. 42 °C)[13] are moderate to low-melting solids, and are termed as ionic liquids. The well known trihexyl(tetradecyl)phosphonium chloride (CYPHOS IL 101), available on the ton scale for more than a decade, is liquid at room temperature, which is the case of most of the compounds presented here.

[a]*The QUILL Centre, The Queen's University of Belfast, Stranmillis Road, Belfast, UK, BT9 5AG. E-mail: quill@qub.ac.uk*
[b]*Current address: Department of Chemistry, Indian Institute of Technology Madras, Chennai, India, 600 036*
[c]*Instituto de Tecnologia Química e Biológica, Universidade Nova de Lisboa, Oeiras, Portugal, 2780-901; Web: www.itqb.unl.pt*
[d]*Cytec Canada Inc, 9061 Garner Rd., Niagara Falls, Ontario, Canada, L2E 6S5*

The tetraalkylphosphonium ionic liquids, which contain cations with a distorted tetrahedral structure, have not surprisingly very different structural and physical properties to those, say, based on a planar aromatic cation. This has been well illustrated in a recent paper,[14] which predicted a different morphology, and hence different physicochemical properties for each class of ionic liquid.

We present here the first systematic study of a related series of tetralkylphosphonium ionic liquids, producing synthetically pure materials with extensive physicochemical characterisation. An interesting, and with hindsight perhaps predictable, phenomenon which emerged from this work was the observation of the effect of the "even/odd" number of carbons in the fourth alkyl chain on the physical properties. Systematic studies involving changes in the alkyl substitution on the cation and/or the anion, have been previously reported in the literature.[15] However, we believe principally for reasons of cost, published studies have largely focussed on cations containing alkyl chains with an even number of carbon atoms; of these the majority have focussed on 1,3-dialkylimidazolium salts. Of these, remarkably few studies have included alkyl chains containing both even and odd number of carbon atoms.[16–18]

Experimental

Instrumental

Autoclave. The miniclave drive manufactured by Büchi Glas Uster (Switzerland) was purchased from Ken Kimbel & Co. Ltd. (United Kingdom). The autoclave consists of a glass reactor with nominal volume 200 cm^3; holder for glass reactor with stainless steel anti-splinter cage; insert ring; cover plate with 6 welded-in $\frac{1}{4}$" Swagelok connections, welded on bmd 075 magnetic drive; O-ring seal; union nut and holding rod. The magnetic coupling (bmd 075) is combined with the cyclone 075 (0–2500 rpm) equipped with an electric motor, into a hermetically sealed unit. The controller is equipped with a remote control input for external speed adjustment. The stationary housing of the magnetic drive and the cover plate are welded together and built as one common unit. The cover plate contains pressure relief valve, platinum resistance thermometer (Pt 100), gas inlet tube, pressure gauge and an inlet/outlet tube. The maximum temperature is 250 °C and maximum pressure is 10 bar.

Microwave. MicroSYNTH microwave used was manufactured by Milestone (Italy) as the single-mode set up with a 20 cm^3 volume vial placed in the TMF safety shield vessel, closed by TMF screw cap and located in the microwave cavity (43 l) at the position with the highest energy intensity allowing rapid heating. Reaction temperature control is provided by an IR sensor (max. 250 °C), monitoring the outside surface temperature of the vessel, mounted in the sidewall of the cavity, about 5 cm above the bottom and fibre-optic sensor (max. 300 °C) immersed within the vessel. A pneumatic pressure sensor (max. 55 bar) placed inside the vessel monitors the vapour concentration and overall pressure. An additional sensor monitors the pressure inside the cavity. Post-reaction cooling of the reaction mixture is achieved by a constant airflow (1.8 m^3 min^{-1}) through the cavity and a stream of compressed air. The MicroSYNTH reaction system is monitored *via* an external control terminal with a touch screen display utilising the EasyControl 640 software package. The run can be controlled either by temperature, pressure or microwave output (max. 1000 W). The software enables on-line modifications of any method parameter and the reaction process is monitored by an appropriate graphical interface. Agitation is achieved by magnetic stirring (max. 400 rpm) controlled by software.

NMR spectroscopy. All NMR spectra were recorded on a Bruker Advance spectrometer DPX 300 at 21 °C, using deuteriated propanone as solvent (10–20 mM solutions for ^{1}H and ^{31}P NMR spectroscopy; 30–35 mM solutions for ^{13}C NMR spectroscopy), referred to TMS for ^{1}H and ^{13}C NMR spectra and 85% H_3PO_4 for ^{31}P NMR spectra.

Mass spectrometry. Most samples were analysed by fast atom bombardment (FAB) spectrometry, performed on with VG-Autospec (Fisons Instruments) in a positive ion mode. Two of the samples ($[P_{8889}]Cl$ and $[P_{88814}]Cl$) were analysed by electrospray ionisation mass spectrometry (ESI-MS) on a Waters LCT Premier mass spectrometer (Micromass Technologies).

Microanalysis. Elemental carbon and hydrogen contents (wt%) were analysed using a Perkin–Elmer Series II CHNS/O 2400 CHN Elemental Analyser, and provided analysis within ±0.3 wt% error. Halide content was determined by dioxygen flask, combustion followed by halide titration with aqueous mercury(II) nitrate, using a dicarbazide indicator.

Water content. Water content was determined using a Cou-Lo Compact (version 08.05) Karl Fischer titrator, and titration solutions from Riedel-de-Haën. Ionic liquids were tested immediately after drying under high vacuum for 48 h, and the water content was below 450 ppm for all samples.

Differential scanning calorimetry (DSC). The melting points and glass transitions of the compounds were measured by DSC, using a TA Instruments Modulated DSC Q 2000 V24.4 Build 116 with refrigerated cooling system RCS 90 capable of controlling the temperature down to 220 K. Dry dinitrogen gas was purged through the DSC cell with a flow rate of *ca.* 20 cm^3 min^{-1}. All samples, due to their hygroscopic character, were prepared in a glove box, using Tzero hermetic platinum pans to avoid any contact with air and measured under the same conditions (standard heating and cooling ramp of 5 K min^{-1} over five cycles).

Thermogravimetric analysis (TGA). Decomposition temperature measurements were performed in a TA Instruments Q50 thermogravimetric analyser. The samples were measured in platinum pans, at a heating rate of 10 K min^{-1}, in a dynamic mode, under a dinitrogen atmosphere. The onset of weight loss in each thermogram was used as a measure of decomposition temperature (see Results and Discussion). The sample size was typically between 7 and 10 mg and sample preparation was similar to that described for the DSC measurements.

Density measurements. Density was measured with an Anton Paar vibrating tube densimeter, model DMA 4500, operating at atmospheric pressure and within the temperature range 273 to 363 K. The internal calibration of the instrument was confirmed by measuring densities of atmospheric air and doubly distilled water, according to the recommendations of the manufacturer. The DMA 4500 cell was embedded in a metallic block, the temperature

of which was controlled by several Peltier units. This arrangement enabled a temperature stability better than ±2 mK.

All ionic liquids used in density determinations were degassed under vacuum and moderate temperature conditions for periods longer than 48 h and were injected into the densimeter immediately after cooling, using non-lubricated disposable syringes.

Viscosity measurements. The viscosity was determined using an AMVn microviscometer, Anton Paar, that allows measurements from 273 to 363 K at atmospheric pressure, and over a wide viscosity range (0.3 to 20 000 mPa s). A glass capillary with 4 mm internal diameter and a 3 mm gold/tungsten ball (placed inside the capillary) of density 15 g cm^{-3} was chosen for this study and an extension of runtime up to 1000 s was required due to the high viscosity of each sample. Temperature was maintained constant to within ±0.01 K by a capillary block with in-built Peltier elements. Since these ionic liquids were extremely hygroscopic, the capillary was always charged in the glove box. The capillary/ball system was calibrated with standard viscosity oil (1 Pa s) from PRA. Viscosity measurements were performed in steps of 10 K from 293 K up to 363 K for all ionic liquid samples for which a sufficient amount (*ca.* 3.5 cm^3) was available. Each sample was measured ten times in order to check reproducibility.

Glove box. All ionic liquids studied here were handled in a dinitrogen-filled glove box (MBraun LabMaster dp; 0.1 ppm < O_2 and H_2O) immediately after drying, and stored there until used.

Materials

The phosphonium ionic liquids presented in this study were synthesised following the procedures described in the next section. Chloromethane (≥99.5%), chloroethane (≥99.7%), 1-chloropropane (98%), 1-chlorobutane (99.5%), 1-chloropentane (99%), 1-chlorohexane (99%), 1-chloroheptane (99%), 1-chlorooctane (99%), 1-chlorononane (98%), 1-chlorodecane (98%), 1-chlorododecane (98%) and 1-chlorotetradecane (98%) were all purchased from Aldrich and used as received. Trioctylphosphine (97%, $\rho = 0.859$ g cm^{-3}) was supplied by Cytec Industries, Canada.

Synthetic procedures

Three different techniques were used to synthesise alkyltrioctylphosphonium chlorides. An autoclave was used for reactions with volatile gaseous chloroalkanes such as chloromethane and chloroethane. Syntheses of $[P_{8883}]Cl$ and $[P_{8884}]Cl$, which used chloroalkanes of mid-range volatility, were performed in a microwave reactor and the remaining compounds requiring non-volatile chloroalkanes were synthesised *via* thermal reflux. Glassware used in the synthetic procedures was charged with starting materials in an M size Atmosbag® (purchased from Sigma Aldrich) which was filled with dinitrogen, in order to provide an inert atmosphere and avoid potential oxidation of the trioctylphosphine to trioctylphosphine oxide. Details of individual syntheses are given in Table 1, elemental analytical data are reported in Table 2. In all cases products were characterised by ^{31}P, ^{13}C and ^{1}H NMR spectroscopy (Tables 4 and 5; Fig. 2) and by mass spectrometry (Tables 2 and 3) prior to purification.

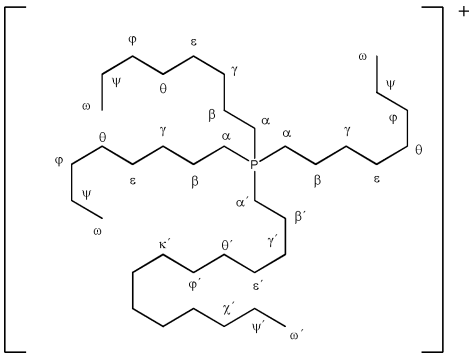

Fig. 2 Numbering convention used for the cation described in the ^{1}H, ^{13}C and ^{31}P NMR tables. The fourth (variable) alkyl substitution on the phosphorus is labelled as a secondary chain (α′, β′, γ′, *etc.*) where the terminal position takes priority, apart from positions α′ and β′.

Synthesis of $[P_{888n}]Cl$, n = 1 or 2. The autoclave glass reactor was charged with trioctylphosphine (see Table 1) under a dinitrogen atmosphere, placed into the stainless steel cage holder, and quickly attached to the cover plate. A gas cylinder containing chloroalkane (chloromethane or chloroethane) was connected to the autoclave through the gas inlet tube. The gas and inlet valves were opened after the set up was proved to be tight and the gas flow was maintained at 2 cm^3 min^{-1}. The reaction mixture was slowly heated over several hours in an oil bath until the temperature inside of the reactor reached 145 °C. The pressure in the reactor was built up by an excess of chloroalkane and did not exceed 4 bar with increasing temperature. The gas inlet was closed after approximately one hour and the reaction was maintained at 145 °C for two hours in the case of chloromethane, and for an additional two hours in the case of chloroethane. After the reaction was cooled down to room temperature, the pressure was released, and a sample for ^{31}P NMR spectroscopy was taken to check for the disappearance of the phosphine signal. The content of the reactor was then transferred to a round-bottomed flask (100 cm^3) and dried at 65 °C *in vacuo* for 48 h.

Synthesis of $[P_{888n}]Cl$, n = 3 or 4. Trioctylphosphine (1 mol eq.) was mixed with chloroalkane (1.1 mol eq.) in a 20 cm^3 glass microwave vial with inserted stirring bar, under an inert atmosphere (dinitrogen). The reaction mixture was transferred under Suba-Seal® septa (purchased from Sigma Aldrich) avoiding any contact with air while transferring from the Atmosbag® to the shield vessel. The septum was removed and discarded immediately before the TMS screw cap was attached to the shield vessel. They were then placed inside the microwave cavity. The reaction conditions were: Ramp (5 min) to 180 °C; hold at 180 °C (30 min), medium stirring, 500 W (50% max) power; pressure reached 3 bar. After the reaction was completed and cooled down, the product was transferred to a round-bottomed flask (25 cm^3) and dried at 65 °C *in vacuo* for 48 h.

Synthesis of $[P_{888n}]Cl$, n = 5–9, 10, 12 or 14. Trioctylphosphine (1 mol eq.) and chloroalkane (1.1 mol eq.) were placed in a round-bottomed flask (50 cm^3). The mixture was stir-heated under a reflux condenser connected to the Schlenk line flushed with dinitrogen. The reaction mixture was heated in a silicone oil bath up to 145 °C and maintained from 12 to 16 h depending on the alkyl chain length of chloroalkane used. In order to remove the

Table 1 Masses of reactants (m), reaction conditions for synthesis, yield, appearance and water content of $[P_{888n}]Cl$ ionic liquids

	P_{888}		$C_nH_{2n+1}Cl$								
n	V/cm^3	m/g	V/cm^3	m/g	ρ/g cm^{-3} [a]	T/°C	t/h	Yield/%	Colour	State[b]	H_2O/ppm
1	72.73	60	32.80	30	0.915	140[c]	2.5[c]	92	White	s	—
2	72.73	60	32.70	30	0.918	140[c]	4.5[c]	94	Pale yellow	s	—
3	12.12	10	2.61	2.33	0.892	180[d]	0.5[d]	96	Colourless	l	442
4	12.12	10	3.10	2.78	0.886	180[d]	0.5[d]	97	Colourless	l	425
5	12.12	10	3.59	3.16	0.882	145	12	96	Colourless	l	411
6	12.12	10	4.10	3.58	0.879	145	12	94	Colourless	l	395
7	12.12	10	4.54	4.00	0.881	145	14	95	Colourless	l	340
8	12.12	10	5.04	4.41	0.875	145	14	96	Colourless	l	296
9	14.55	12	6.66	5.80	0.870	145	16	95	Colourless	l	256
10	12.12	10	6.04	5.25	0.868	145	16	95	Colourless	l	233
12	12.12	10	7.00	6.08	0.867	145	16	92	Colourless	l	225
14	12.12	10	8.05	6.91	0.859	145	16	89	Pale yellow	l	218

[a] Density data provided by supplier. [b] s = solid; l = liquid. [c] Synthesis performed in autoclave. [d] Synthesis performed in microwave.

Table 2 Elemental analysis of $[P_{888n}]Cl$ and identification of cations by +ve FAB-MS, where peaks were assigned as $[P_{888n}]^+$

	C/%		H/%		Cl/%		P/%		m/z	
n	calc.	exp.	calc.	exp.	calc.	exp.	calc.	exp.	calc.	exp.
1	71.30	71.36	12.92	12.72	8.42	8.48	7.36	7.44	385.4	385.5
2	71.76	71.70	12.97	12.12	8.15	8.44	7.35	7.74	399.4	399.4
3	72.20	72.06	13.02	13.28	7.89	7.43	6.90	7.23	413.4	413.4
4	72.60	72.76	13.06	13.09	7.65	8.08	6.69	6.07	427.4	427.2
5	72.99	72.17	13.09	13.38	7.43	7.89	6.49	6.56	441.4	441.2
6	73.35	73.35	13.13	12.84	7.22	7.90	6.30	5.91	455.4	455.2
7	73.69	73.26	13.17	13.21	7.02	7.61	6.13	5.92	469.5	469.3
8	74.01	73.63	13.20	13.60	6.83	7.13	5.96	5.64	483.5	483.3
9	74.32	73.65	13.23	13.62	6.65	6.61	5.81	5.42	—	—
10	74.61	74.82	13.26	13.65	6.48	6.52	5.66	5.01	511.5	511.3
12	75.14	74.89	13.31	13.02	6.16	5.95	5.38	6.14	539.5	539.3
14	75.63	75.13	13.36	13.23	5.87	6.43	5.13	5.21	—	—

Table 3 $[P_{8889}]Cl$ and $[P_{88814}]Cl$ were identified by electrospray ionisation spectrometry (ESI-MS)

	$\{[P_{888n}]Cl_2\}^-$			$[P_{888n}]^+$		
n	ES^-_{theo}	ES^-_{exp}	relative intensity %	ES^+_{theo}	ES^+_{exp}	relative intensity %
9	567.5, 568.5 569.5, 570.5 571.5, 572.5	567.5, 568.5 569.5, 570.5 571.6, 572.5	100, 25 55, 15 3, 2	497.5, 498.5, 499.5	497.5, 498.6, 499.5	100, 38, 5
14	—	—	—	567.6, 568.6, 569.6	567.6, 568.6, 569.6	100, 40, 5

excess of starting 1-chloroalkane ($C_nH_{2n+1}Cl$), where $n \geq 5$, the purification step involved dissolution of the product in hexane, followed by extraction with water. All products were dried *in vacuo* for 48 h.

Results and discussion

Synthetic procedures

The tetralkylphosphonium chlorides studied here, were prepared by nuclephilic (S_N2) addition of a trialkylphosphine to linear chloroalkanes varying from chloromethane to chlorotetradecane:

$$P_{888} + C_nH_{2n+1}Cl \xrightarrow[\text{no solvent}]{S_N2} [P_{888n}]^+Cl^-$$

Alkylphosphines are often compared to their analogous amines,[19] which are an integral part of the synthetic construction units of ionic liquids, although there are few similarities between them when it comes to chemical reactivity. Some of the underlying differences are the excellent nucleophilicity of alkylphosphines[20] towards electro-positive carbon due to their relatively low ionisation energies (favouring electron transfer); increased strength of carbon-phosphorus bonds; and the larger size and higher polarisability of the phosphorus atom leading to a lower repulsion energy during the reaction, despite of the fact that the pK_a of trioctylphosphine (9.58) is lower than that of trioctylamine (10.82).[21] Nucleophilic attack of phosphorus at a haloalkane, RX, depends on the reactivity of the haloalkane, which decreases with increasing C–X bond strength in a sequence: RF < RCl < RBr < RI. This explains why in this work all the syntheses

Table 4 For $[P_{888}{}_n]Cl$, ^1H NMR shifts (δ/ppm, d_6-propanone, 300 MHz, 21 °C), with coupling constant ($^2J_{PH}$/Hz) and $^{31}P\{^1H\}$ NMR shifts (δ/ppm, d_6-propanone, 120 MHz, 21 °C); peaks were assigned according to Fig. 2

	$H^{\alpha,\alpha'}$		$H^{\beta,\beta'}$		$H^{\gamma,\gamma'\text{-}\psi,\psi'}$		$H^{\omega,\omega'}$		^{31}P
n	δ/ppm	intensity	δ/ppm	intensity	δ/ppm	intensity	δ/ppm	intensity	δ/ppm
1	2.44–2.54 (m), 2.05 (d, J = 14.1)	6H,3H$^{(\alpha')}$	1.50–1.63 (m)	6H	1.06–1.30 (m), 1.33–1.42 (m)	24H,6H	0.74–0.79 (m)	9H	33.46
2	2.51–2.63 (m)	8H	1.50–1.64 (m)	6H	1.12–1.30 (m), 1.32–1.44 (m)	27H,6H	0.74–0.78 (m)	9H	36.24
3	2.49–2.57 (m)	8H	1.52–1.63 (m)	8H	0.95–0.98 (m), 1.32–1.44 (m)	3H,24H	0.74–0.77 (m)	9H	34.12
4	2.52–2.64 (m)	8H	1.50–1.63 (m)	8H	0.82–0.86 (m), 1.14–1.29 (m), 1.32–1.44 (m)	3H,24H,8H	0.74–0.78 (m)	9H	34.47
5	2.45–2.55 (m)	8H	1.43–1.56 (m)	8H	1.05–1.35 (m)	34H	0.66–0.74 (m)	12H	34.47
6	2.53–2.63 (m)	8H	1.50–1.65 (m)	8H	1.07–1.42 (m)	36H	0.74–0.84 (m)	12H	34.44
7	2.50–2.60 (m)	8H	1.51–1.63 (m)	8H	1.10–1.41 (m)	38H	0.74–0.78 (m)	12H	34.45
8	**2.52–2.62 (m)**	**8H**	**1.50–1.60 (m)**	**8H**	**1.10–1.42 (m)**	**40H**	**0.74–0.78 (m)**	**12H**	**34.46**
9	2.49–2.59 (m)	8H	1.50–1.61 (m)	8H	1.11–1.41 (m)	42H	0.74–0.80 (m)	12H	34.49
10	2.64–2.74 (m)	8H	1.65–1.78 (m)	8H	1.25–1.55 (m)	44H	0.88–0.92 (m)	12H	34.43
12	2.65–2.75 (m)	8H	1.65–1.77 (m)	8H	1.25–1.45 (m),1.48–1.54 (m)	40H,8H	0.88–0.92 (m)	12H	34.43
14	2.46–2.56 (m)	8H	1.50–1.63 (m)	8H	1.13–1.28 (m),1.32–1.41 (m)	46H,8H	0.73–0.78 (m)	12H	34.42

Table 5 For $[P_{888}{}_n]Cl$, $^{13}C\{^1H\}$ NMR shifts (δ/ppm, d_6-propanone, 75 MHz, 21 °C), with coupling constants ($^1J_{PC}$/Hz), peaks were assigned according to Fig. 2

	$C^{\alpha,\alpha'}$	$C^{\beta,\beta'}$	$C^{\gamma,\gamma'}$	$C^{\varepsilon,\varepsilon',\theta,\theta'}$	$C^{\kappa'\text{-}\chi'}$	$C^{\varphi,\varphi'}$	$C^{\psi,\psi'}$	$C^{\omega,\omega'}$
n	δ/ppm	δ/ppm	δ/ppm	δ/ppm	δ/ppm	δ/ppm	δ/ppm	δ/ppm
1	5.10(d, J_{PC} = 51.75 Hz), 21.27(d, J_{PC} = 48.75 Hz)	23.79	30.30	32.10, 31.90		33.04	22.68	14.90
2	13.71(d, J_{PC} = 48.75 Hz), 19.63(d, J_{PC} = 47.10 Hz)	23.88, 6.90	30.15	32.22, 32.02		33.04	22.83	14.88
3	19.92(d, J_{PC} = 47.18 Hz), 21.92(d, J_{PC} = 47.25 Hz)	23.76, 16.68	30.07	32.16, 31.96		33.00	22.73	14.82, 16.37
4	19.75(d, J_{PC} = 47.40 Hz), 19.96(d, J_{PC} = 47.18 Hz)	24.82, 23.78	30.10	32.19, 31.99		33.01	22.78, 25.17	14.85, 14.30
5	19.97(d, J_{PC} = 47.18 Hz)	23.78, 23.13	30.11,34.01	32.20, 31.99		33.02	22.83, 22.48	14.85, 14.65
6	19.99(d, J_{PC} = 47.18 Hz)	23.78, 23.59	30.13, 31.79	32.21, 32.01		33.03	22.87	14.87
7	19.99(d, J_{PC} = 47.10 Hz)	23.80	30.16	32.85, 32.00, 32.21		33.04	22.84	14.89
8[a]	**19.99(d, J_{PC} = 47.10 Hz)**	**23.80**	**30.23**	**32.22, 32.12**		**33.05**	**22.85**	**14.89**
9	19.96(d, J_{PC} = 47.10 Hz)	23.78	30.34	32.18, 31.98, 30.49$^{\theta'}$		33.02	22.80	14.85
10	19.96(d, J_{PC} = 47.25 Hz)	23.77	30.28	32.18, 31.97, 30.72$^{\theta',\varphi'}$		33.02	22.80	14.84
12	19.98(d, J_{PC} = 47.18 Hz)	23.78	30.33	32.19, 31.99	30.84	33.02	22.81	14.84
14	20.01(d, J_{PC} = 47.03 Hz)	23.83	30.16	32.24, 32.04	30.35, 30.94	33.08	22.88	14.92

[a] Due to the symmetry of the compound, all the peak assignments are equal.

presented were carried out under harsh reaction conditions (high temperature, long reaction time). Taking into account the twelve basic rules of green chemistry (specifically, rule number five, which states: "The use of auxiliary substances (*e.g.* solvents, separation agents, *etc.*) should be made unnecessary wherever possible and innocuous when used")[22] and the impact of the solvent on reaction time, the solvent was excluded from all synthetic procedures. Reaction time depends also on the number of carbon atoms in the chloroalkane; the longer the alkyl chain length, the longer the reaction takes. Syntheses performed in the microwave reactor were much more time and energy efficient compared to conventional heating methods. This methodology can be applied to any organic reaction, regardless of the volatility of starting compounds, and reaches even higher efficiency using software for predicting and optimising yields as developed by Strauss.[23] The average yield for all synthesised compounds was 94%, with purification being the yield reducing step. The purification step was performed to remove the excess of chloroalkane from the product and consisted in the dissolution of the ionic liquid in hexane followed by washing with water and further drying *in vacuo* for 48 h. Almost all products were colourless, with just two exceptions ($[P_{8882}]Cl$ and $[P_{88814}]Cl$), which had a pale yellow colour even after purification. The whole series is hydrophobic, giving two phases when mixed with water.

Nuclear magnetic resonance spectroscopy

^{31}P NMR. The $^{31}P\{^1H\}$ NMR spectra of $[P_{888}{}_n]Cl$ (see Table 4) all exhibited a singlet at +34.40 ± 0.33 ppm with the exceptions of $[P_{8881}]Cl$ and $[P_{8882}]Cl$, where the signals were at +33.46 ppm and +36.24 ppm, respectively. Often the singlet is accompanied by minor peaks, each of similar intensity, on either side as the result of the presence of more than one active nucleus, in this case ^{13}C nuclei ("spin–spin splitting"), see Fig. 3. The distance between adjacent peaks around singlet is a measure of the strength of the interaction and is denoted by a coupling constant, $^1J_{PC}$, which was 62.42 ± 0.46 Hz for all compounds studied here.

As the free trioctylphosphine signal is at –29.51 ppm, monitoring of the reactions is very straightforward. For accurate

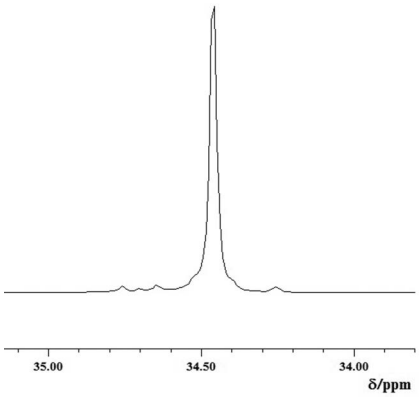

Fig. 3 $^{31}P\{^{1}H\}$ NMR spectrum of $[P_{8888}]Cl$ in d_6-propanone.

interpretation of ^{31}P NMR of phosphonium ionic liquids, it is important to know the purity of starting phosphine (Fig. 4).

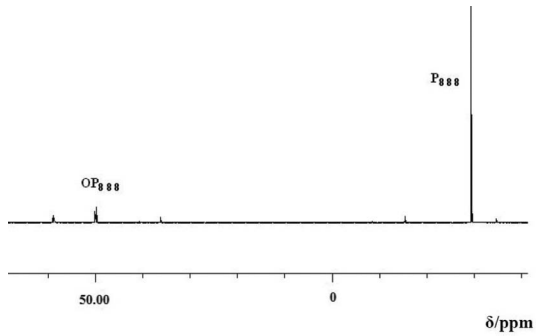

Fig. 4 $^{31}P\{^{1}H\}$ NMR spectrum (d_6-propanone, 120 MHz, 21 °C) with peak assignments of trioctylphosphine, and its corresponding phosphine oxide.

Trioctylphosphine is industrially prepared (Cytec, Canada) by free radical addition[24] of PH_3 to 1-octene. This process results in the formation of two isomeric tertiary phosphine by-products. The major isomeric impurity originates from a Markovnikov addition[25] to the secondary carbon of 1-octene. This isomer, di(1-octyl)(2-octyl)phosphine, typically accounts for 2.5 to 3.0% of the tertiary octylphosphines and has a clearly visible down-field chemical shift as indicated in the ^{31}P NMR spectra of the commercially supplied trioctylphosphine, see Fig. 4. The 1-octene used above also has traces (<1%) of a branched 1-octene isomer. Addition to this olefin results in the formation of another, but relatively minor tertiary phosphine which has a chemical shift slightly up-field from that of the main component (–34.63 ppm). The spectrum also reveals the presence of a small amount of trioctylphosphine oxide (as the trialkylphosphines are easily oxidised when exposed to air[26]). Trace amounts of dioctyl octylphosphonate $[O{=}P(C_8H_{17})(OC_8H_{17})_2]$, another air oxidation product, can be detected as well. The percentage of the trioctylphosphine isomers do not exceed more than 3% in the starting material. The above tertiary alkylphosphine isomers are also quaternised along with the tri(1-octyl)phosphine analogue. The corresponding phosphonium salt derived from di(1-octyl)(2-octyl)phosphine has a ^{31}P NMR chemical shift slightly further down-field from that of the main component (+38.60 ± 0.22 ppm and +34.40 ± 0.33 ppm, respectively). The main component phosphonium salt and its isomers account for > 98% of the phosphorus.

^{1}H and ^{13}C NMR. The cationic charge has a strong influence on the electron density around the hydrogen atoms close to the cationic centre, therefore their shifts can be observed at high magnetic field. In comparison with the corresponding ammonium-based ionic liquids, phosphonium ionic liquids are more stable. The difference in shifts of protons closest to the cationic center is *ca.* 1 ppm downfield compared to ammonium based ionic liquids.[27]

A major difference in chemical shifts of protons can be observed with increasing number of carbon atoms in the fourth alkyl chain on the cation. The protons of the methyl substituent (Fig. 5-A) in $[P_{8881}]Cl$ can be observed as doublet due to the strong phosphorus–hydrogen interaction.

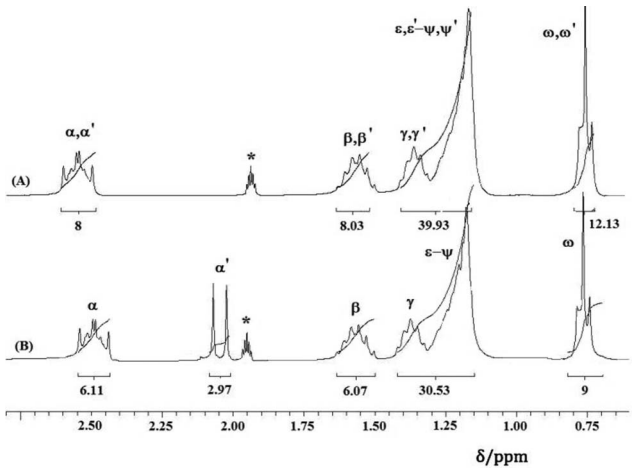

Fig. 5 ^{1}H NMR spectra(d_6-propanone, 120 MHz, 21 °C) of (A) $[P_{8888}]Cl$ and (B) $[P_{8881}]Cl$, peaks are assigned according to Fig. 2 (individual peaks are assigned in Table 4), solvent is assigned as (*).

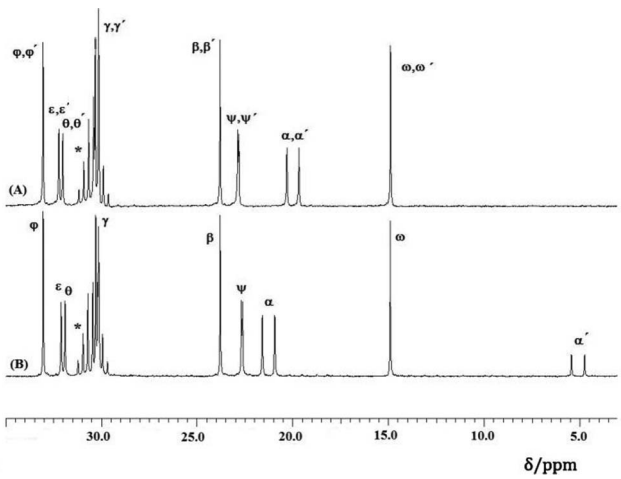

Fig. 6 $^{13}C\{^{1}H\}$ NMR spectra (d_6-propanone, 120 MHz, 21 °C) of (A) $[P_{8888}]Cl$ and (B) $[P_{8881}]Cl$, peaks are assigned according to Fig. 3 (individual peaks are assigned in Table 5), solvent is assigned as (*).

As the number of methylene groups increases, the shift of the methyl group at the end of the fourth alkyl substitution moves towards to lower magnetic field until reaches the multiplet

belonging to methyl groups of three remaining octyl substitutions on the cation, Fig. 5 (see Table 4). The sensitivity of the chemical shift of the terminal methyl group as a function of chain length is noted, see Table 5 and Fig. 6.

Differential scanning calorimetry measurements and thermogravimetric analysis

The melting and glass transition temperatures were measured by differential scanning calorimetry. The values of the melting temperature (T_m) and glass transition (T_g) are shown in Table 6 for all compounds investigated. The trend of T_m or T_g as a function of the number of carbon atoms in the fourth alkyl substitution on the phosphonium cation is displayed in Fig. 7.

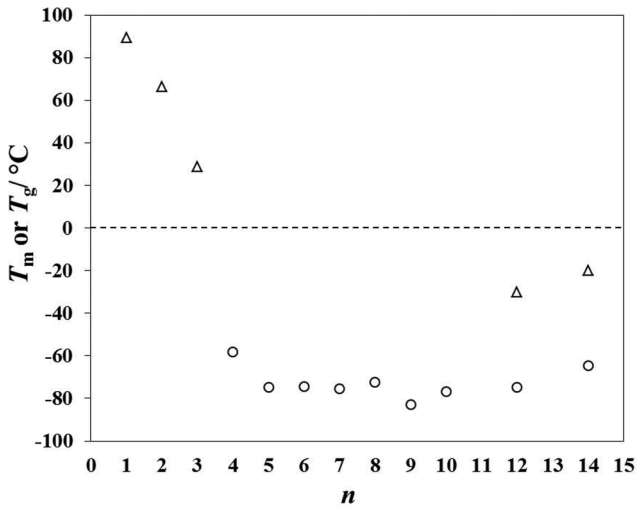

Fig. 7 Melting (△) and glass transition (○) temperatures, T_m and T_g, respectively, as a function of the number of carbons, n, in the fourth alkyl substituent on the phosphonium cation.

Table 6 Decomposition temperatures, T_d for $[P_{888n}]Cl$ were determined by dynamic TGA. T_m and T_g obtained by DSC are reported along with the enthalpies of fusion, ΔH_{fus}, and enthalpies of glass transition, $\Delta H_{glass\text{-}l}$

n	T_m/°C	ΔH_{fus}/J g^{-1}	T_g/°C	$\Delta H_{glass\text{-}l}$/J g^{-1}	T_d/°C
1	89.3	8.49	—	—	323
2	66.2	20.87	—	—	317
3	28.6	31.24	—	—	322
4	—	—	−58.2	0.65	326
5	—	—	−74.9	0.78	310
6	—	—	−74.6	0.97	305
7	—	—	−75.4	0.36	315
8	—	—	−72.5	1.12	317
9	—	—	−82.8	2.82	295
10	—	—	−77.0	0.24	312
12	−30.0	9.96	−74.8	0.09	320
14	−20.0	13.33	−64.5	0.05	330

The melting point is taken as the onset of an endothermic peak on heating and the glass transition temperature is taken as the midpoint of a small heat flow change on heating from the amorphous glass state to a liquid state. Two examples of DSC scans are presented in Fig. 8.

Most of the studied compounds simply form a glass at low temperatures with no apparent freezing or melting transitions.

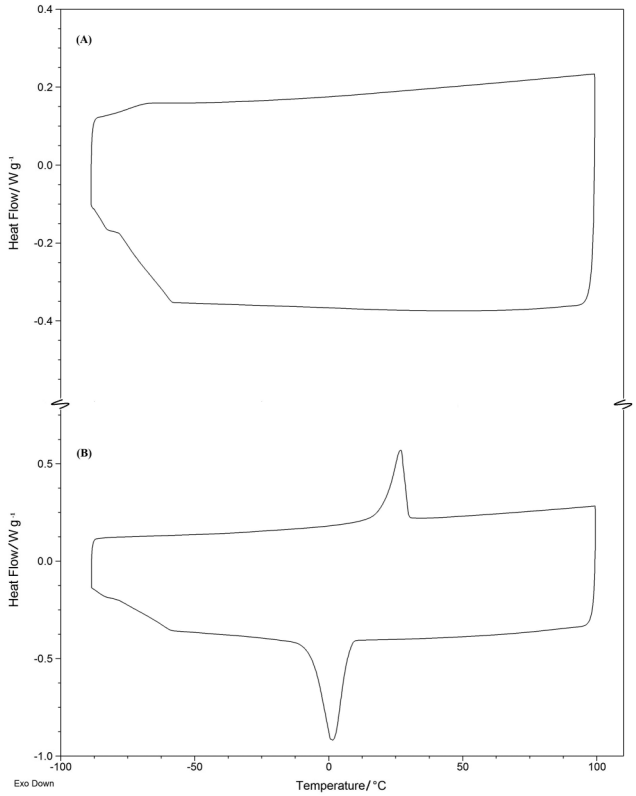

Fig. 8 DSC scans of (A) $[P_{8887}]Cl$ and (B) $[P_{8883}]Cl$, scan speed 5 K min^{-1}.

The glass transition temperatures are in the range of −82.8 °C ($[P_{8889}]Cl$) to −58.2 °C ($[P_{8884}]Cl$). Samples that were solids at room temperature displayed distinct melting peaks, specifically compounds with n = 1–3. This is probably due to the small size of the cation which leads to closer cation anion contact which in turn produces a higher lattice energy.[28] It was already reported by Tindale *et al.*[29] that, as the alkyl chain length is increased on the cation (Me < Bu < Oct) for the series of iodide salts, the melting point decreases. Our findings agree with their results. The ionic liquids with the longest chain (n = 12 or 14) are liquid at room temperature, but exhibit observable melting points as well as glass transition points.

Unlike their ammonium counterparts, which tend to undergo facile Hoffmann- or β-elimination in the presence of base,[30] phosphonium salts decompose to yield a tertiary phosphine oxide and an alkane under alkaline conditions.[31] In contrast, tetralkylphosphonium halides can be combined with concentrated sodium hydroxide well above room temperature without any degradation.[32] While the decomposition point of neat phosphonium ionic liquid varies with the counter ion,[7] the alkyltrioctylphosphonium chlorides under investigation here, appear to show dynamic onset of decomposition at around 320 ± 20 °C (data are reported in Table 6, and typical TGA scans are shown in Fig. 9). Pyridinium-based salts,[33] in contrast, decompose at about 100 °C higher temperature.

Density and molar volume

Density measurements were carried out over a broad range of temperatures (293.15 < T/K < 363.15) at atmospheric pressure, and data are reported along with the corresponding molar volume,

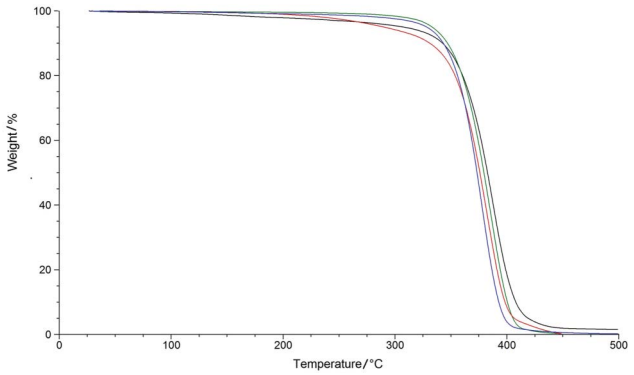

Fig. 9 Typical TGA curves for $[P_{888n}]Cl$, examples of $[P_{8881}]Cl$ (black line), $[P_{8884}]Cl$ (green line), $[P_{8888}]Cl$ (red line) and $[P_{88812}]Cl$ (blue line).

V_m, for each studied ionic liquid in Table 7. The repeatability of the density measurements was better than 5×10^{-5} g cm^{-3}.

The densities of the investigated compounds are in the range of 0.84 to 0.90 g cm^{-3} over a temperature range of 293.15 to 363.15 K. It is commonly well known, that tetraalkylphosphonium halides have densities below 1 g cm^{-3}; the longer the alkyl chains on the cation, the less dense the phosphonium ionic liquids become. Obviously, the choice of the anion has a big impact on the density,[34] chlorides showing a lower density in comparison to other anions such as triflate, $[OTf]^-$; bistriflamide, $[NTf_2]^-$; tetrafluoroborate, $[BF_4]^-$; or hexafluorophosphate, $[PF_6]^-$; when paired with the same cation.[7] On average, the decrease in density is 4.4% for an increase in temperature from 293.15 to 363.15 K.

The plot of experimental densities for $[P_{888n}]Cl$, as a function of n, is shown in Fig. 10. The density decreases with increasing chain length. The even-numbered compounds form a *quasi*-straight line, while the odd-numbered compounds deviate from this line showing another, independent *quasi*-linear behaviour. This leads to an apparent alternation effect observed up to $[P_{8889}]Cl$ (see red line in Fig. 11). Fig. 11 also indicates that, when the density data are partitioned into three sets (n = even up to 8, odd up to 9, and $n > 9$), then each of these sets lie upon a straight line as a function of n, all with very high regression coefficients ($R^2 > 0.995$). The discontinuity observable for $n \geq 10$ corresponds well to the phase

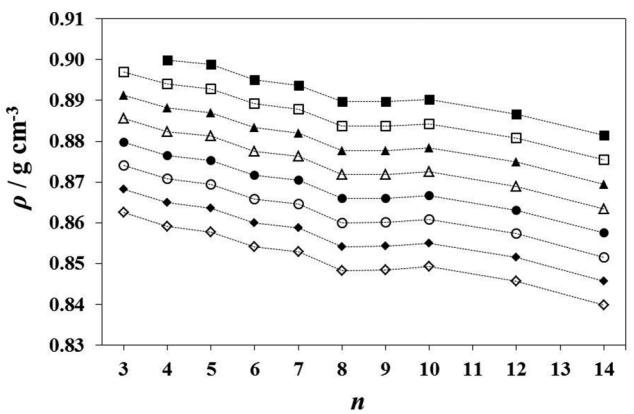

Fig. 10 Experimental densities for $[P_{888n}]Cl$ ionic liquids at 293 K (■), 303 K (□), 313 K (▲), 323 K (△), 333 K (●), 343 K (○), 353 K (◆) and 363 K (◇) as a function n. Experimental data for compounds, where $n = 1$ or 2 are not included as they are solids with melting points above 65 °C.

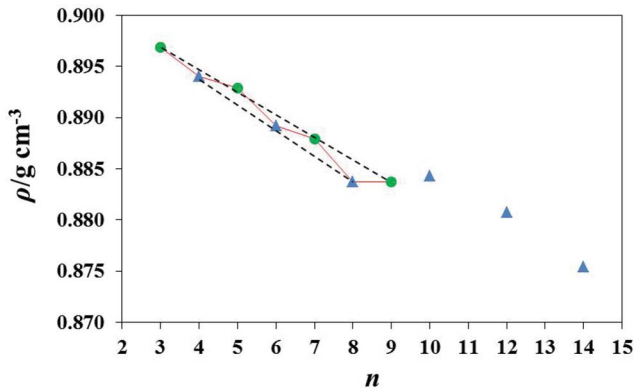

Fig. 11 Experimental densities of $[P_{888n}]Cl$ ionic liquids at 30 °C, where $n = 3$, 5, 7 and 9 (●), $n = 4$, 6, 8, 10, 12 and 14 (▲).

diagram illustrated in Fig. 7, which for $n > 10$ shows both T_g and T_m transitions, indicating the onset of a different structural régime.

In the temperature range studied, the density decreases *quasi*-linearly with increasing temperature as illustrated in Fig. 12.

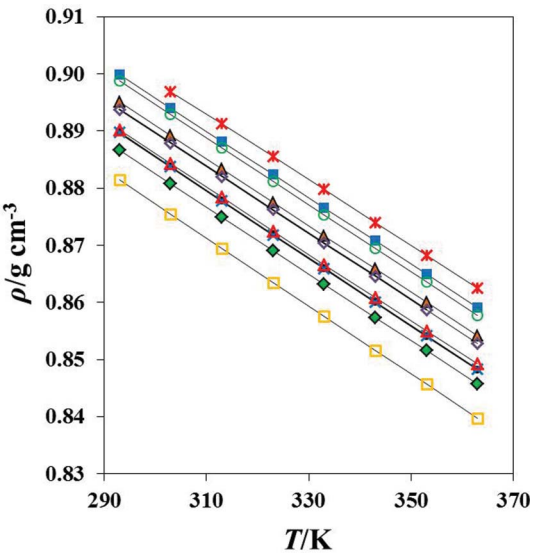

Fig. 12 Experimental density as a function of temperature for the $[P_{888n}]Cl$ ionic liquids series where $n = 3$ (×), 4 (■), 5 (○), 6 (▲), 7 (◊), 8 (●), 9 (×), 10 (△), 12 (♦) and 14 (□). The lines correspond to the linear fit of experimental results obtained in this work ($0.99998 \leq R^2 \leq 1$).

It is also of interest to express the volumetric behaviour of phosphonium ionic liquids in terms of their molar volume, $V_m = M/\rho$, where an expected increase of V_m with increasing temperature is observed, see Fig. 13. V_m as a function of n exhibits a *quasi*-linear trend for each represented temperature, Fig. 14. A detailed analysis of the residuals of the data from Fig. 14 for $3 \leq n \leq 9$, see Fig. 15, clearly shows the see-saw, alternation, odd/even effect, which had also been observed in the densities, see Fig. 11. Examination of Fig. 10 and 11 suggests a non-linear response of density (the empirical parameter) to chain length; the deviations from linearity are small, but significant. In examining the molar volumes (the thermodynamically significant parameter), see Fig. 14, the regular deviation from linearity is much smaller and therefore can only been revealed unambiguously on the residuals plotted in Fig. 15.

Table 7 Experimental density (ρ/g cm^{-3}) and molar volume (V_m/cm^3 mol^{-1}) data for [P_{888n}]Cl ionic liquids measured at temperatures T = 293.15 K to T = 363.15 K. Calculated density values were obtained from the extended Ye and Shreeve equation[35] proposed by Gardas and Coutinho.[36] ΔV_m values represent the difference (calc – exp) between V_m values and molar volume data calculated using the fitting eqn (6)

T/K	ρ_{exp}/ g cm^{-3}	ρ_{calc}/ g cm^{-3}	Dev[a]/%	$(V_m)_{exp}$/ cm^3 mol^{-1}	$(V_m)_{calc}$/ cm^3 mol^{-1}	ΔV_m[b]/ cm^3 mol^{-1}	T/K	ρ_{exp}/ g cm^{-3}	ρ_{calc}/ g cm^{-3}	Dev[a]/%	$(V_m)_{exp}$/ cm^3 mol^{-1}	$(V_m)_{calc}$/ cm^3 mol^{-1}	ΔV_m[b]/ cm^3 mol^{-1}
[P_{8883}]Cl							**[P_{8884}]Cl**						
293.15	—	—	—	—	—	—	293.15	0.8998	0.8977	−0.24	514.78	513.47	−1.31
303.15	0.8969	0.8938	−0.35	500.83	499.98	−0.85	303.15	0.8940	0.8917	−0.25	518.15	517.22	−0.93
313.15	0.8912	0.8879	−0.37	504.01	503.65	−0.36	313.15	0.8882	0.8858	−0.26	521.54	520.97	−0.57
323.15	0.8855	0.8821	−0.39	507.25	507.32	0.07	323.15	0.8824	0.8800	−0.27	524.95	524.72	−0.23
333.15	0.8798	0.8763	−0.39	510.57	510.99	0.42	333.15	0.8766	0.8743	−0.26	528.44	528.47	0.03
343.15	0.8740	0.8707	−0.38	513.94	514.65	0.71	343.15	0.8707	0.8686	−0.24	531.97	532.22	0.25
353.15	0.8683	0.8651	−0.37	517.35	518.32	0.97	353.15	0.8649	0.8631	−0.22	535.55	535.96	0.41
363.15	0.8625	0.8596	−0.34	520.79	521.99	1.20	363.15	0.8591	0.8576	−0.18	539.16	539.71	0.55
[P_{8885}]Cl							**[P_{8886}]Cl**						
293.15	0.8988	0.8957	−0.34	530.98	530.63	−0.35	293.15	0.8951	0.8939	−0.13	548.87	547.78	−1.09
303.15	0.8929	0.8898	−0.35	534.48	534.46	−0.02	303.15	0.8892	0.8880	−0.14	552.49	551.69	−0.80
313.15	0.8870	0.8839	−0.35	538.02	538.29	0.27	313.15	0.8833	0.8821	−0.14	556.15	555.60	−0.55
323.15	0.8812	0.8781	−0.35	541.57	542.12	0.55	323.15	0.8775	0.8763	−0.14	559.82	559.52	−0.30
333.15	0.8753	0.8724	−0.34	545.20	545.95	0.75	333.15	0.8717	0.8706	−0.12	563.58	563.43	−0.15
343.15	0.8695	0.8668	−0.31	548.88	549.78	0.90	343.15	0.8658	0.8650	−0.10	567.39	567.34	−0.05
353.15	0.8636	0.8612	−0.28	552.61	553.61	1.00	353.15	0.8600	0.8594	−0.06	571.25	571.25	−0.00
363.15	0.8578	0.8557	−0.24	556.37	557.44	1.07	363.15	0.8542	0.8540	−0.03	575.14	575.16	0.02
[P_{8887}]Cl							**[P_{8888}]Cl**						
293.15	0.8938	0.8922	−0.18	565.35	564.94	−0.41	293.15	0.8897	0.8905	0.09	583.70	582.09	−1.61
303.15	0.8879	0.8862	−0.19	569.09	568.93	−0.16	303.15	0.8837	0.8846	0.10	587.65	586.17	−1.48
313.15	0.8820	0.8804	−0.19	572.87	572.92	0.05	313.15	0.8778	0.8788	0.12	591.64	590.24	−1.40
323.15	0.8762	0.8746	−0.18	576.66	576.92	0.26	323.15	0.8719	0.8730	0.13	595.64	594.31	−1.33
333.15	0.8704	0.8689	−0.17	580.54	580.91	0.37	333.15	0.8659	0.8674	0.17	599.74	598.39	−1.35
343.15	0.8645	0.8633	−0.14	584.47	584.90	0.43	343.15	0.8600	0.8617	0.20	603.87	602.46	−1.41
353.15	0.8587	0.8578	−0.11	588.45	588.89	0.44	353.15	0.8541	0.8562	0.25	608.06	606.54	−1.52
363.15	0.8529	0.8523	−0.06	592.48	592.89	0.41	363.15	0.8482	0.8507	0.30	612.27	610.61	−1.66
[P_{8889}]Cl							**[P_{88810}]Cl**						
293.15	0.8897	0.8890	−0.08	599.45	599.25	−0.20	293.15	0.8902	0.8876	−0.30	614.90	616.40	1.50
303.15	0.8837	0.8831	−0.07	603.50	603.40	−0.10	303.15	0.8843	0.8817	−0.30	619.01	620.64	1.63
313.15	0.8778	0.8773	−0.06	607.60	607.56	−0.04	313.15	0.8784	0.8759	−0.29	623.16	624.88	1.72
323.15	0.8718	0.8715	−0.03	611.76	611.71	−0.05	323.15	0.8725	0.8701	−0.27	627.38	629.11	1.73
333.15	0.8659	0.8658	−0.01	615.92	615.87	−0.05	333.15	0.8666	0.8645	−0.25	631.61	633.35	1.74
343.15	0.8601	0.8602	−0.02	620.11	620.03	−0.08	343.15	0.8608	0.8589	−0.23	635.87	637.59	1.72
353.15	0.8542	0.8547	−0.06	624.36	624.18	−0.18	353.15	0.8550	0.8534	−0.20	640.19	641.83	1.64
363.15	0.8483	0.8493	−0.11	628.67	628.34	−0.33	363.15	0.8492	0.8479	−0.16	644.57	646.06	1.49
[P_{88812}]Cl							**[P_{88814}]Cl**						
293.15	0.8866	0.8849	−0.20	649.01	650.71	1.70	293.15	0.8814	0.8825	0.12	684.67	685.02	0.35
303.15	0.8807	0.8790	−0.20	653.36	655.21	1.85	303.15	0.8754	0.8766	0.13	689.35	689.58	0.23
313.15	0.8749	0.8732	−0.19	657.72	659.51	1.79	313.15	0.8694	0.8708	0.16	694.13	694.15	0.02
323.15	0.8690	0.8675	−0.17	662.20	663.91	1.71	323.15	0.8634	0.8651	0.20	698.93	698.71	−0.22
333.15	0.8631	0.8618	−0.15	666.67	668.31	1.64	333.15	0.8575	0.8595	0.23	703.75	703.27	−0.48
343.15	0.8573	0.8563	−0.12	671.19	672.71	1.52	343.15	0.8516	0.8539	0.27	708.65	707.84	−0.81
353.15	0.8515	0.8508	−0.09	675.77	677.11	1.34	353.15	0.8457	0.8484	0.33	713.61	712.40	−1.21
363.15	0.8457	0.8453	−0.04	680.42	681.51	1.09	363.15	0.8398	0.8430	0.39	718. 63	716.96	−1.67

[a] Dev (%) = $[(\rho_{calc} - \rho_{exp})/\rho_{exp}] \times 100$. [b] $\Delta V_m = (V_m)_{calc} - (V_m)_{exp}$.

Experimental density data were fitted into the extended Ye and Shreeve equation[35] proposed by Gardas and Couthino,[36] which is applicable over a wide range of temperatures 273–393 K, and pressures, 0.10–100 MPa, according to eqn (1):

$$\rho_{IL}(T,P) = M/N_A V^{mol}(a + bT + cP) \quad (1)$$

where M is the formula mass in g mol^{-1}, N_A is the Avogadro's number, V^{mol} is the molecular volume in units of 1×10^{-27} cm^3, T is the temperature in K, and P is the pressure in MPa. The values of the coefficients a, b and c were estimated by Gardas and Coutinho[36] as 0.80050 ± 0.00023, $(6.6520 \pm 0.0069) \times 10^{-4}$ K^{-1}, and $(-5.919 \pm 0.024) \times 10^{-6}$ MPa^{-1}, respectively, by fitting eqn (1) to the previously published experimental pressure–volume–temperature (PVT) data of ILs.[37,38]

The densities of alkyltrioctylphosphonium ionic liquids were estimated according to eqn (1) with the molecular volumes of ions and groups taken from previously reported values[36,39,40] where available. Since a range of values for the molecular volume of the chloride ion have ben published previously, in this work the value was estimated by minimising the objective function (OF), given in eqn (2):

$$OF = \sum_{i=1}^{N_p} (\rho_{calc} - \rho_{exp})^2 / N_p \quad (2)$$

where ρ_{calc} is calculated density using eqn (1), ρ_{exp} is the experimental density, and N_p represents the number of data points, in this case $N_p = 79$. The calculated density ρ_{calc} of the studied ionic liquids

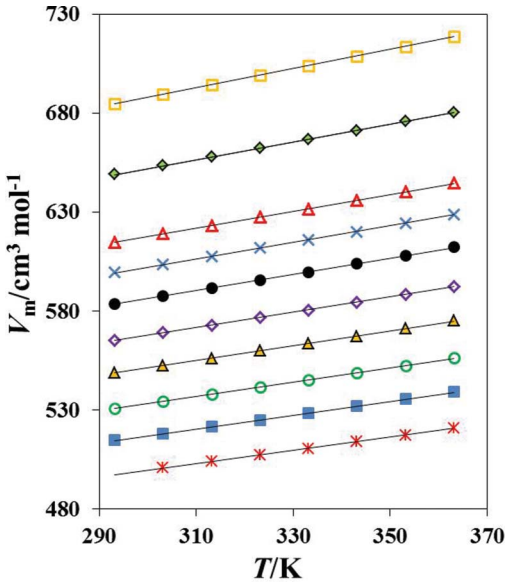

Fig. 13 Molar volumes as a function of temperature for the $[P_{888n}]Cl$ ionic liquids series where n = 3 (×), 4 (■), 5 (○), 6 (▲), 7 (♡), 8 (●), 9 (×), 10 (△), 12 (♦) and 14 (□). The lines correspond to the linear fit of experimental results obtained in this work ($0.99998 \leq R^2 \leq 1$).

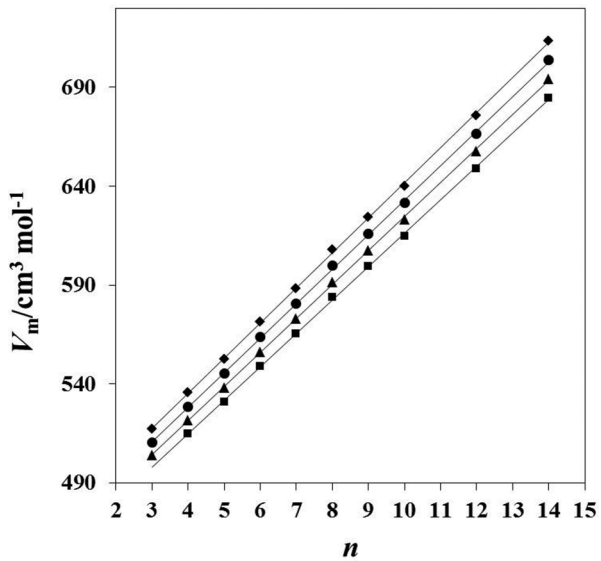

Fig. 14 Experimental molar volume of $[P_{888n}]Cl$ as a function of n for four temperatures. The isotherms are 293 K (■), 313 K (▲), 333 K (●) and 353 K (◆). The lines represent a linear fit of the results for each isotherm.

displays a good agreement with the corresponding experimental density ρ_{exp}, where (see Fig. 16):

$$\rho_{calc} = (0.9988 \pm 0.0002)\rho_{exp}$$

(R^2 = 0.9849 at a 95% level of confidence)

For the density prediction from molar volume, using eqn (1), an average absolute deviation (AAD) of 0.2% with the maximum deviation (MD) 0.39% was observed for 79 density data points studied of 10 ionic liquids, where AAD is defined as, eqn (3):

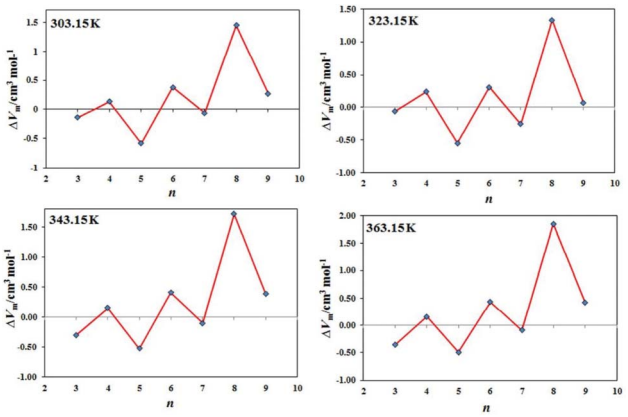

Fig. 15 Illustration of the see-saw, even/odd alternation effect in the form of deviations (residuals) between experimental and fitted data as a function of n, at four different temperatures.

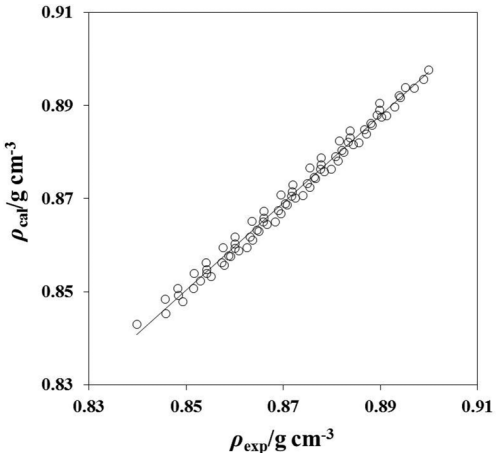

Fig. 16 Linear relationship between experimental and calculated density of herein studied ionic liquids at temperatures T = 293.15 K to T = 363.15 K, using the extended Ye and Shreeve equation proposed by Gardas and Coutinho.

$$\text{AAD (\%)} = \sum_{i=1}^{N_p} \left| \frac{\rho_{calc} - \rho_{exp}}{\rho_{exp}} \right| \Big/ N_p \qquad (3)$$

Rebelo and coworkers[41] used a simplified model to predict the molar volumes of three phosphonium ionic liquids, which share the same cation ($[P_{66614}]^+$) and different anions.

An "ideal" volumetric behaviour[33,42–45] was previously observed for 1-alkyl-3-methylimidazolium-based ionic liquids, where a high degree of linearity was noted in the plots of molar volume (V_m) *vs.* the number of carbon atoms in the alkyl chain (n). The variation of the molar volume per addition of two carbon atoms in the cation of these ionic liquids, $(\partial V_m/\partial(2n))$ = (34.4 ± 0.5) cm^3 mol^{-1} was obtained, irrespective of the anion and the length of the chain. Equally important, this rule-of-thumb is observed irrespective of whether the chains are incorporated in either the cation or the anion. A striking case is that of the 1-alkyl-3-methylimidazolium alkylsulfonates,[15] where the observed linearity as n increases enabled the establishment of effective volumes ("molar size") occupied by all the other anions and cations. The molar volume (V_m) of an ionic liquid was defined simply as the

sum of the effective molar volumes (V^*) of the anion (a) and cation (c), eqn (4):

$$V_m = V_c^* + V_a^* \quad (4)$$

This model,[41] the first totally predictive in nature once an anchor anion (or cation) is chosen, was developed based on density data obtained at 298.15 K. Following the logic of Rebelo and coworkers,[41] any cations with the same empirical formulae should have the same molar volumes, irrespective of how the alkyl chain lengths are distributed around central phosphorus. Thus, the molar volume of $[P_{888n}]Cl$ should equal that of $[P_{666(n+6)}]Cl$ at any temperature, and hence the extant calculated molar volume of $[P_{66614}]Cl$ (582.5 cm^3 mol^{-1} at 298.15 K)[41] should serve as a fair estimate for the molar volume of $[P_{8888}]Cl$. In fact, the experimental value obtained in this work deviates by only 0.5% from this value. If this model is applied to the data reported here, although reasonable fits may be obtained, the precision of these data is greater than the difference between estimated and observed values and hence, the differences are statistically significant; this phenomenon will be discussed in detail elsewhere, alongside data for related series of ionic liquids.[46]

For the first time, we would like to introduce a group contribution method for the prediction of molar volume as a function of temperature. The phosphonium ionic liquids presented in this study were divided into three groups, see Fig. 17, and each group is represented as a function of temperature according to the following eqn (5):

$$V_m(G_i) = A + B(T - 273.15) \quad (5)$$

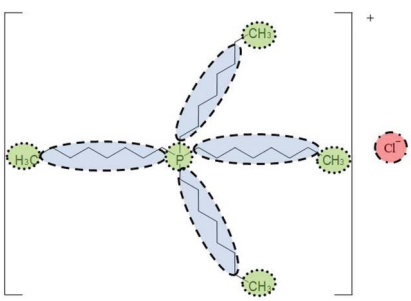

Fig. 17 Structure of $[P_{8888}]Cl$ divided into groups, distinguished by colours (red, blue and green), representing molar volumes of each moiety, G_i (i = 1, 2, or 3).

V_m relates to the structure, Fig. 17, and is considered to be composed of contributions from $[P_{1111}]^+$ (green), $-(CH_2)_n-$ (blue) and Cl^- (red), hence the overall molar volume is represented by eqn (6):

$$V_m = \sum_{i=1}^{3} V_m(G_i) \quad (6)$$

The parameters A and B can be obtained by a group contribution method according to eqn (7) and eqn (8):

$$A = \sum_{i=1}^{3} n_i a_i \quad (7)$$

Table 8 Group contribution parameters associated with eqn (5) used to predict the effective molar volume of the phosphonium ionic liquids as a function of temperature from 293.15 to 363.15 K

G_i	a_i/cm^3 mol^{-1}	b_i/cm^3 mol^{-1} K^{-1}
$[P_{1111}]^+$	73.776	0.0840
$-CH_2-$	16.992	0.0082
Cl^-	24.391	0.0954

Table 9 AAD and MD observed for the molar volumes of studied phosphonium ionic liquids predicted using eqn (6)

n	AAD/%	MD/%
3	0.13	0.23
4	0.10	0.25
5	0.13	0.20
6	0.07	0.20
7	0.05	0.07
8	0.25	0.28
9	0.02	0.06
10	0.26	0.28
12	0.24	0.27
14	0.09	0.23

$$B = \sum_{i=1}^{3} n_i b_i \quad (8)$$

where n_i is the number of groups of type i, and the parameters a_i and b_i here estimated are presented in Table 8.

Calculated molar volumes are in an excellent agreement with the corresponding experimental values $(V_m)_{exp}$, where:

$$(V_m)_{cal} = (1.0003 \pm 0.0002) \times (V_m)_{exp}$$

(R^2 = 0.9997 at 95% level of confidence)

The relative deviations between the calculated and experimental data as a function of experimental molar volume for all data points used in the current study are shown in Fig. 18 and 19, similar behaviour to that seen in Fig. 15. For 79 data points of twelve phosphonium ionic liquids, the overall AAD is 0.13% and MD is 0.28% (Table 9).

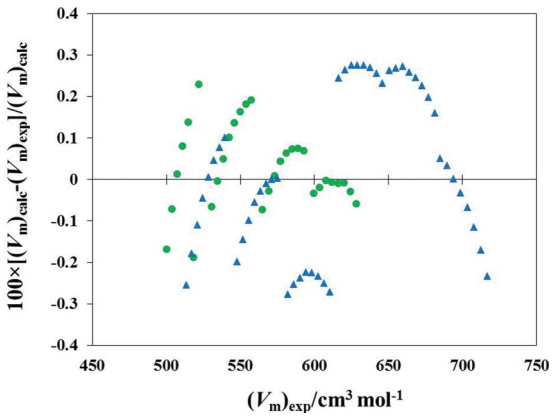

Fig. 18 The relative deviations between calculated, using eqn (5) and the experimental molar volumes as a function of experimental molar volumes for the phosphonium ionic liquids, where n = 3, 5, 7 and 9 (●) and n = 4, 6, 8, 10, 12 and 14 (▲).

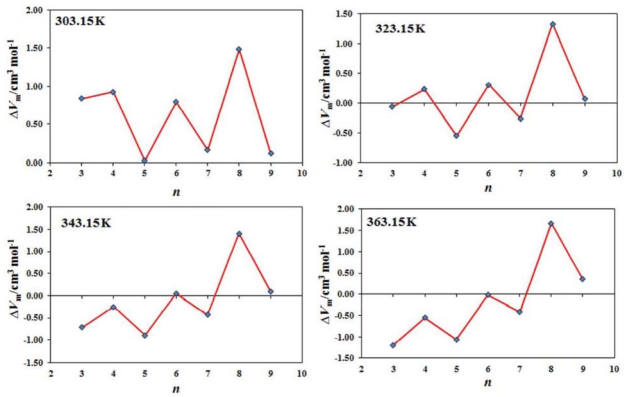

Fig. 19 Illustration of the see-saw, even/odd alternation effect in the form of deviations (residuals) between experimental and predicted data according to eqn (6) as a function of *n*, at four different temperatures.

As shown in the density section, the variation between odd and even number of carbons in the fourth alkyl substitution (*n*) on the cation causes non-linear behaviour. It is satisfying to observe the internal consistency between the data plotted in Fig. 15 and that presented in Fig. 19, given the different assumptions made in the data treatment.

Thermal expansion coefficient

The evolution of the volumetric properties with temperature can be expressed by calculating the coefficient of thermal expansion, α_p, defined as, eqn (9):

$$\alpha_p = -[\partial \ln(\rho)/\partial T]_p = -a \quad (9)$$

Plots of ln(ρ) as a function of temperature, eqn (10), (fitting equation parameters can be found in Table 10) for the studied ionic liquids form *quasi*-linear lines and they are also quite parallel to each other, therefore, the thermal expansion coefficient, α_p, is almost constant.

$$\ln[(\rho/\mathrm{cm}^{-3})] = a(T/\mathrm{mK}) + b \quad (10)$$

In very high-accuracy measurements over an enlarged temperature range, Tariq *et al.*[17] demonstrated that on the homologous series of [C$_n$mim][NTf$_2$], α_p may slightly decrease with increasing temperature in the low-T region, to start increasing (also mildly) in the high-T domain. Additionally, there is a tendency for an increase of α_p with the alkyl chain length. In our present study, a similar behaviour was found: within our studied [P$_{888n}$]Cl family, the calculated values of α lie between 6.52×10^{-4} K^{-1} and 6.91×10^{-4} K^{-1}, for [P$_{8883}$]Cl and [P$_{88814}$]Cl, respectively.

Table 10 Parameters of the linear fit, according to eqn (10)

n	$\alpha_p = -a/\mathrm{K}^{-1} \times 10^{-3}$	*b*
3	0.65213	0.089049
4	0.66716	0.089011
5	0.66926	0.084025
6	0.67984	0.082484
7	0.67505	0.077658
8	0.66079	0.088278
9	0.66787	0.085060
10	0.68262	0.083352
12	0.67314	0.081092
14	0.69145	0.076565

$\bar{\alpha}_p = (6.72 \pm 0.11) \times 10^{-4}$ K^{-1}

This is significantly lower than the α_p values of common, molecular organic liquids – and it is not at all surprising since a typical ionic liquid at these working temperatures is at a considerably lower hypothetical reduced temperature[47,17] than any common low-molecular weight organic liquid. Values of α_p of the same order of magnitude ($5–6 \times 10^{-4}$ K^{-1}) were reported by Gu and Brennecke[48] for several ionic liquids containing [BF$_4$]$^-$ and [PF$_6$]$^-$ anions and imidazolium and pyridinium-based cations. The only two literature references dealing with the thermal expansion coefficient of phosphonium ILs, are those of (i) Esperança *et al.*[41] who studied [P$_{66614}$]$^+$ in combination with three different anions ([NTf$_2$]$^-$/[O$_2$CMe]$^-$/Cl$^-$) obtaining 6.70×10^{-4} K^{-1}, 6.19×10^{-4} K^{-1}, and 6.04×10^{-4} K^{-1}, respectively, while (ii) Tariq *et al.*[34] with [NTf$_2$]$^-$/[OTf]$^-$/[O$_2$CMe]$^-$ obtained 6.91×10^{-4} K^{-1}, 6.69×10^{-4} K^{-1}, and 6.83×10^{-4} K^{-1}, respectively.

Viscosity

Factors that affect viscosity of ionic liquids are still not fully understood, but the chemical structure of the anion is known to have a strong influence. Specifically halides have high viscosity as they likely take part in hydrogen bonding.[49] The viscosity can be decreased by addition of water or organic solvent.[42]

Viscosities were measured at temperatures between 293.15 to 363.15 K for ten phosphonium ionic liquids out of the twelve presented here (see Table 11); the limitation is their liquid range. The results indicate that the viscosity of the studied phosphonium ionic liquids decreases markedly with temperature increase, for example, on increasing temperature by 10 K from (293.15 to 303.15) K one observes a decrease in viscosity for [P$_{8888}$]Cl of 51%. The decrease in viscosity observed was up to 98% by increasing the temperature from 293.15 to 363.15 K. Viscosity as a function of the fourth alkyl chain is illustrated in Fig. 20. To the best of our knowledge, this is the first time that it is observed that, on average, the viscosity decreases (although only modestly) with increasing alkyl chain length.

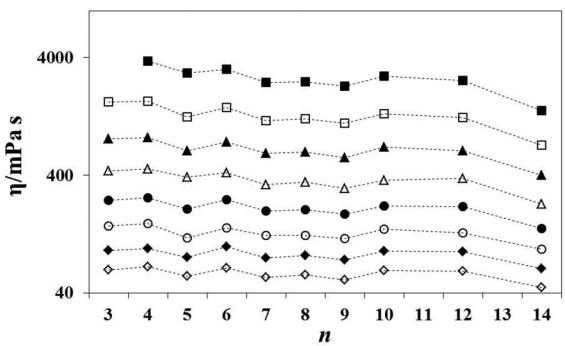

Fig. 20 Experimental viscosities of [P$_{888n}$]Cl ionic liquids at 293.15 K (■), 303.15 K (□), 313.15 K (▲), 323.15 K (△), 333.15 K (●), 343.15 K (○), 353.15 K (◆) and 363.15 K (◇) as a function of the number of carbon atoms in the alkyl chain of the fourth alkyl substitution on the cation.

Having established this behaviour which shows both an alternation effect and unexpected chain length dependence, the reasons for this behaviour will be discussed elsewhere.[46]

Table 11 Experimental viscosities (η_{exp}) of phosphonium chlorides as a function of temperature at atmospheric pressure. Dev[a] represents standard deviation of ten measurements performed with each sample at each given temperature. Calculated viscosities (η_{cal}) were obtained from the VFT equation and AAD represents agreement between calculated and experimental data

T/K	η_{exp}/mPa s	Dev/%	η_{cal}/mPa s	AAD/%	T/K	η_{exp}/mPa s	Dev/%	η_{cal}/mPa s	AAD/%
[P_{8883}]Cl					**[P_{8884}]Cl**				
293.15	—	—	—	—	293.15	3732.66	1.54	3732.66	0.00
303.15	1682.00	1.92	1667.50	0.86	303.15	1708.15	2.58	1695.46	0.74
313.15	812.45	2.55	827.66	1.87	313.15	839.82	2.73	841.51	0.20
323.15	436.34	2.51	442.57	1.43	323.15	449.98	4.38	449.98	0.00
333.15	245.28	2.08	252.10	2.78	333.15	258.62	4.75	256.32	0.89
343.15	148.67	1.93	151.59	1.96	343.15	155.35	3.23	154.12	0.79
353.15	91.19	1.27	95.50	2.48	353.15	95.26	2.63	97.10	1.93
363.15	62.59	1.03	62.65	0.10	363.15	66.82	2.19	63.70	4.67
[P_{8885}]Cl					**[P_{8886}]Cl**				
293.15	2964.65	0.93	2705.17	8.75	293.15	3190.71	1.98	3190.69	0.00
303.15	1245.15	1.70	1272.95	2.23	303.15	1509.85	2.94	1506.48	0.22
313.15	641.65	2.55	650.80	1.43	313.15	768.46	2.74	772.36	0.51
323.15	385.12	4.39	356.83	7.35	323.15	422.01	3.11	424.50	0.59
333.15	206.69	2.08	207.66	0.47	333.15	247.54	1.73	247.54	0.00
343.15	116.95	2.18	127.18	8.75	343.15	143.41	2.73	151.88	5.91
353.15	80.32	3.70	81.42	1.37	353.15	98.77	2.04	97.37	1.41
363.15	55.59	0.86	54.16	2.56	363.15	65.17	1.56	64.87	0.46
[P_{8887}]Cl					**[P_{8888}]Cl**				
293.15	2455.34	2.77	2455.35	0.00	293.15	2488.28	1.80	2488.28	0.00
303.15	1156.30	2.98	1176.12	1.71	303.15	1202.16	2.33	1200.96	0.10
313.15	616.10	4.98	610.35	0.93	313.15	629.05	3.37	627.22	0.29
323.15	334.51	5.21	338.92	1.32	323.15	348.42	2.76	350.18	0.50
333.15	199.66	1.86	199.39	0.13	333.15	204.88	3.40	206.97	1.02
343.15	123.27	3.25	123.27	0.00	343.15	122.52	2.94	128.47	4.85
353.15	79.28	3.31	79.55	0.35	353.15	83.21	4.22	83.20	0.02
363.15	54.18	1.03	53.30	1.63	363.15	57.07	2.88	55.92	2.02
[P_{8889}]Cl					**[P_{88810}]Cl**				
293.15	2286.52	1.62	2286.52	0.00	293.15	2775.56	4.65	2759.52	0.58
303.15	1102.62	2.13	1104.14	0.14	303.15	1322.93	2.31	1322.93	0.00
313.15	565.36	1.72	576.65	2.00	313.15	694.44	5.33	687.02	1.07
323.15	309.30	1.94	321.95	4.09	323.15	361.63	1.47	381.73	5.56
333.15	187.86	0.61	190.28	1.29	333.15	219.74	1.66	224.68	2.25
343.15	115.82	2.89	118.11	1.98	343.15	138.84	4.16	138.97	0.09
353.15	76.35	3.80	76.49	0.19	353.15	90.43	0.82	89.72	0.78
363.15	51.37	6.48	51.41	0.07	363.15	61.80	0.87	60.13	2.69
[P_{88812}]Cl					**[P_{88814}]Cl**				
293.15	2539.44	1.64	2516.87	0.89	293.15	1411.34	1.59	1468.29	4.03
303.15	1233.02	3.74	1233.02	0.00	303.15	719.37	2.09	719.37	0.00
313.15	644.20	2.21	652.12	1.23	313.15	398.69	3.67	388.08	2.66
323.15	377.48	3.82	368.00	2.51	323.15	227.43	1.88	226.35	0.47
333.15	215.65	2.22	219.51	1.79	333.15	14.,53	3.11	140.77	0.17
343.15	129.29	2.89	137.33	6.22	343.15	93.98	2.82	92.34	1.75
353.15	89.57	1.93	89.56	0.01	353.15	64.32	2.58	63.35	1.52
363.15	60.85	1.26	60.55	0.48	363.15	44.30	2.50	45.14	1.90

The Vogel–Fulcher–Tammann equation has been successfully used to model the temperature dependence of ionic liquid viscosity for many years.[2,50] A viscosity–temperature correlation based on the (VFT) equation, eqn (11) is proposed:

$$\eta = A + \exp\left(\frac{B}{T - T_0}\right) \tag{11}$$

where η is the viscosity in mPa s units, T is temperature (K), A, B and T_0 are adjustable parameters. Experimental viscosity as a function of temperature for the three chosen ionic liquids fitted into the VFT equation is presented in Fig. 21.

The ratio of parameters B and T_0, B/T_0, is also known as the Angell strength parameter. Experimental viscosity data of the ionic liquids were used to optimise the parameters A, B and T_0 simultaneously by minimising the following objective function (OF), eqn (12):

$$\mathrm{OF} = \sum_{i=1}^{N_p}\left[A + \frac{B}{T - T_0} - \ln(\rho_{exp})\right]^2 \Big/ N_p \tag{12}$$

The parameters A, B and T_0 of eqn (11) are given in Table 12 together with AAD and MD for the viscosity data of all studied compounds. The values of the parameter T_0 are between 126 to 165 K. Gardas and Coutinho,[51] obtained 165.06 K as T_0 for approximately 500 viscosity data points of 25 imidazolium, pyridinium and pyrrolidinium based ionic liquids.

As shown in Fig. 22, good agreement is observed between calculated and experimental viscosity data using the VFT equation, with all three adjustable parameters (A, B, T_0). The calculated

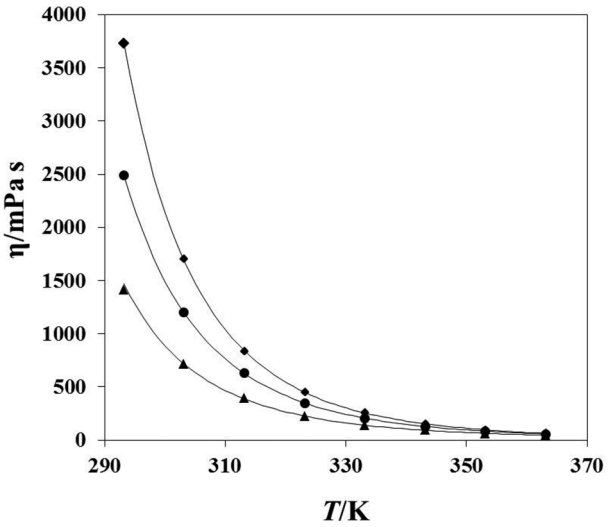

Fig. 21 Experimental viscosities as a function of temperature: $[P_{8884}]Cl$ (◆), $[P_{8888}]Cl$ (●) and $[P_{88814}]Cl$ (▲), fitted into the VFT equation, eqn (11). Fits are represented by solid lines.

Table 12 Correlation parameters of VFT equation with the deviations of the fit for the viscosity of $[P_{888n}]Cl$ as a function of temperature, determined from experimental values in the range $T = 293.15$ to $T = 363.15$ K

n	A	B/K	T_0/K	B/T_0	AAD/%	MD/%
3	−11.95	2095.59	135.12	15.51	2.3	3.7
4	−11.94	2095.59	135.12	15.51	1.2	4.7
5	−11.96	2095.38	131.35	15.95	4.1	8.8
6	−11.76	2095.36	130.98	16.00	1.1	5.9
7	−11.89	2095.29	129.35	16.20	0.8	1.7
8	−11.81	2095.25	128.48	16.31	1.1	4.9
9	−11.90	2095.25	128.48	16.31	1.2	4.1
10	−11.77	2095.27	129.26	16.21	1.6	5.6
12	−11.67	2095.17	126.72	16.53	1.6	6.2
14	−9.47	1263.14	165.00	7.66	1.6	4.0

viscosity (η_{cal}) of studied ILs displays a good agreement with the corresponding experimental viscosity (η_{exp}), Fig. 22, where:

$$\ln(\eta_{cal}) = (0.9929 \pm 0.0035)\ln(\eta_{exp})$$

($R^2 = 0.9992$ at a 95% of confidence)

Relative deviations between the calculated and the experimental viscosity data are presented in Table 11 along with experimental viscosity values at wide range of temperatures (293.15–363.15 K).

Conclusions

A basic synthetic methodology for a series of related phosphonium ionic liquids is presented here, along with a detailed study of their ^1H, ^{13}C and ^{31}P NMR, mass spectra, thermal stability, density and viscosity over a wide range of temperatures, melting points/glass transition temperatures and phase diagrams. For the first time there is evidence for an alternation effect within a series of ionic liquids, which reveals itself in both the density and viscosity data. This is the first series of tetraalkylphosphonium chlorides fully studied and characterised; another two related papers on $[P_{666n}]Cl$ and $[P_{444n}]Cl$ will be submitted shortly. These papers, taken together, significantly expand the range of phosphonium ionic liquids available for potential industrial application, and are significantly more stable than their ammonium analogues.

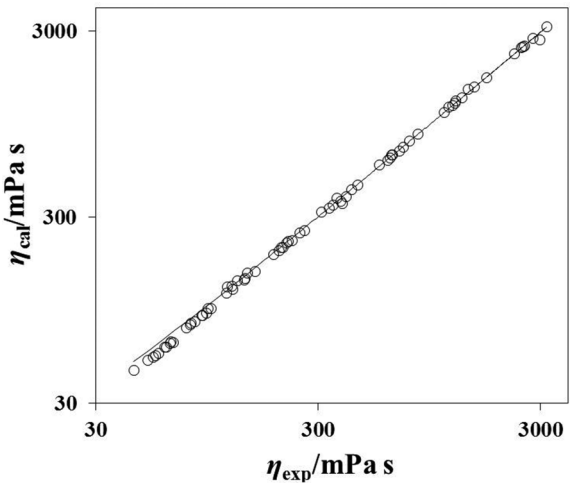

Fig. 22 Linear relationship between η_{exp} and η_{cal} using the VFT equation, eqn (11).

Acknowledgements

This work was funded by Cytec Canada, Inc. G.A. would like to thank Dr Douglas Harris (Cytec) for fruitful comments and advice at the beginning of this work, Dr Marijana Blesic and Dr John Holbrey for countless discussions; Prof. Chris Strauss, Dr Markus Fanselow and Dr Giulia Fiorani for microvawe assistance and helpful guidance. L.P.N.R. thanks *Fundação para a Ciência e Tecnologia* for support under grants PTDC/QUI-QUI/101794/2008 and PTDC/QUI/71331/2006.

Notes and references

1 K. J. Fraser and D. R. MacFarlane, *Aust. J. Chem.*, 2009, **62**, 309–321.
2 K. R. Seddon, A. Stark and M. J. Torres, in *'Clean Solvents - Alternative Media for Chemical Reactions and Processing'* ed. M. A. Abraham and L. Moens, *ACS Symposium Series*, Vol. 819, Am. Chem. Soc., Washington, 2002, pp. 34–49.
3 A. K. Ziyada, C. D. Wilfred, M. A. Bustam, Z. Man and T. Murugesan, *J. Chem. Eng. Data*, 2010, **55**, 3886–3890.
4 S. Seki, T. Kobayashi, Y. Kobayashi, K. Takei, H. Miyashiro, K. Hayamizu, S. Tsuzuki, T. Mitsugi and Y. Umebayashi, *J. Mol. Liq.*, 2010, **152**, 9–13.
5 G. Adamová, R. L. Gardas, L. P. N. Rebelo, A. J. Robertson and K. R. Seddon, *J. Chem. Soc., Dalton Trans.* manuscript in preparation.
6 G. Adamová, R. L. Gardas, M. Nieuwenhuyzen, A. V. Puga, L. P. N. Rebelo, A. J. Robertson and K. R. Seddon, *J. Chem. Soc., Dalton Trans.* submitted.
7 C. J. Bradaric, A. Downard, C. Kennedy, A. J. Robertson and Y. H. Zhou, *Green Chem.*, 2003, **5**, 143–152.
8 Anonymous, 'http://www.cytec.com/specialty-chemicals/phosphine.htm'.
9 R. E. Del Sesto, C. Corley, A. Robertson and J. S. Wilkes, *J. Organomet. Chem.*, 2005, **690**, 2536–2542.
10 N. V. Plechkova and K. R. Seddon, *Chem. Soc. Rev.*, 2008, **37**, 123–150.
11 M. Freemantle, *'An Introduction to Ionic Liquids'*, RSC Publishing, Cambridge, 2010.
12 G. Wittig, *Justus Liebigs Ann. Chem.*, 1953, **580**, 44–57.
13 Anonymous, *'Aldrich Handbook of Fine Chemicals'*, Sigma–Aldrich Chemical Company Ltd.
14 K. Shimizu, M. F. C. Gomes, A. A. H. Padua, L. P. N. Rebelo and J. N. C. Lopes, *THEOCHEM*, 2010, **946**, 70–76.

15 M. Blesic, M. Swadźba-Kwaśny, T. Belhocine, H. Q. N. Gunaratne, J. N. C. Lopes, M. F. C. Gomes, A. A. H. Padua, K. R. Seddon and L. P. N. Rebelo, *Phys. Chem. Chem. Phys.*, 2009, **11**, 8939–8948.
16 M. Tariq, P. J. Carvalho, J. A. P. Coutinho, I. M. Marrucho, J. N. C. Lopes and L. P. N. Rebelo, *Fluid Phase Equilib.*, 2011, **301**, 22–32.
17 M. Tariq, A. P. Serro, J. L. Mata, B. Saramago, J. M. S. S. Esperança, J. N. C. Lopes and L. P. N. Rebelo, *Fluid Phase Equilib.*, 2010, **294**, 131–138.
18 J. D. Holbrey and K. R. Seddon, *J. Chem. Soc., Dalton Trans.*, 1999, 2133–2139.
19 W. A. Henderson and C. A. Streuli, *J. Am. Chem. Soc.*, 1960, **82**, 5791–5794.
20 W. A. Henderson and S. A. Buckler, *J. Am. Chem. Soc.*, 1960, **82**, 5794–5800.
21 ChemAxon, 'www.chemicalize.org', 2010.
22 P. T. Anastas and J. C. Warner, *'Green Chemistry: Theory and Practice'*, Oxford University Press, New York, 1998.
23 C. R. Strauss, *Aust. J. Chem.*, 2009, **62**, 3–15.
24 M. M. Rauhut, H. A. Currier, A. M. Semsel and V. P. Wystrach, *J. Am. Chem. Soc.*, 1961, **26**, 5138–5145.
25 W. Markownikoff, *Justus Liebigs Ann. Chem.*, 1870, **153**, 228–259.
26 S. A. Buckler, *J. Am. Chem. Soc.*, 1962, **84**, 3093–3097.
27 K. Tsunashima and M. Sugiya, *Electrochem. Commun.*, 2007, **9**, 2353–2358.
28 A. F. Kapustinskii, *Q. Rev. Chem. Soc.*, 1956, **10**, 283–294.
29 J. J. Tindale, C. Na, M. C. Jennings and P. J. Ragogna, *Can. J. Chem.*, 2007, **85**, 660–667.
30 J. March, *'Advanced Organic Chemistry'*, 4th Edit., John Wiley and Sons, Inc, New York, 1992.
31 M. Zanger, C. A. Van der Werf and W. E. McEwen, *J. Am. Chem. Soc.*, 1959, **81**, 3806–3807.
32 M. O. Wolff, K. M. Alexander and G. Belder, *Chimica Oggi-Chemistry Today*, 2000, **18**, 29–32.
33 J. M. Crosthwaite, M. J. Muldoon, J. K. Dixon, J. L. Anderson and J. F. Brennecke, *J. Chem. Thermodyn.*, 2005, **37**, 559–568.
34 M. Tariq, P. A. S. Forte, M. F. C. Gomes, J. N. C. Lopes and L. P. N. Rebelo, *J. Chem. Thermodyn.*, 2009, **41**, 790–798.
35 C. F. Ye and J. M. Shreeve, *J. Phys. Chem. A*, 2007, **111**, 1456–1461.
36 R. L. Gardas and J. A. P. Coutinho, *Fluid Phase Equilib.*, 2008, **263**, 26–32.
37 R. L. Gardas, M. G. Freire, P. J. Carvalho, I. M. Marrucho, I. M. A. Fonseca, A. G. M. Ferreira and J. A. P. Coutinho, *J. Chem. Eng. Data*, 2007, **52**, 80–88.
38 R. L. Gardas, M. G. Freire, P. J. Carvalho, I. M. Marrucho, I. M. A. Fonseca, A. G. M. Ferreira and J. A. P. Coutinho, *J. Chem. Eng. Data*, 2007, **52**, 1881–1888.
39 H. D. B. Jenkins, H. K. Roobottom, J. Passmore and L. Glasser, *Inorg. Chem.*, 1999, **38**, 3609–3620.
40 J. Esperanca, H. J. R. Guedes, M. Blesic and L. P. N. Rebelo, *J. Chem. Eng. Data*, 2006, **51**, 237–242.
41 J. M. S. S. Esperança, H. J. R. Guedes, M. Blesic and L. P. N. Rebelo, *J. Chem. Eng. Data*, 2006, **51**, 237–242.
42 K. R. Seddon, A. Stark and M. J. Torres, *Pure Appl. Chem.*, 2000, **72**, 2275–2287.
43 Z. Y. Gu and J. F. Brennecke, *J. Chem. Eng. Data*, 2002, **47**, 339–345.
44 P. A. Z. Suarez, S. Einloft, J. E. L. Dullius, R. F. de Souza and J. Dupont, *J. Chim. Phys. Phys.-Chim. Biol.*, 1998, **95**, 1626–1639.
45 L. P. N. Rebelo, V. Najdanovic-Visak, R.G. de Azevedo, J. M. S. S. Esperança, M. N. da Ponte, H. J. R. Guedes, Z. P. Visak, H. C. de Sousa, J. Szydlowski, J. N. C. Lopes and T. C. Cordeiro, in *'Ionic Liquids IIIA: Fundamentals, Progress, Challenges, and Opportunities, Properties and Structure'*, ed. R. D. Rogers and K. R. Seddon, *ACS Symposium Series*, Vol. 901, Am. Chem. Soc., Washington, 2005, pp. 270–291.
46 G. Adamová, J. N. C. Lopes, L. P. N. Rebelo, A. J. Robertson and K. R. Seddon, *Chem. Sci.* manuscript in preparation.
47 L. P. N. Rebelo, J. N. C. Lopes, J. M. S. S. Esperança and E. Filipe, *J. Phys. Chem. B*, 2005, **109**, 6040–6043.
48 Z. Y. Gu and J. F. Brennecke, *J. Chem. Eng. Data*, 2002, **47**, 339–345.
49 S. A. Forsyth, J. M. Pringle and D. R. MacFarlane, *Aust. J. Chem.*, 2004, **57**, 113–119.
50 A. A. Fannin, D. A. Floreani, L. A. King, J. S. Landers, B. J. Piersma, D. J. Stech, R. L. Vaughn, J. S. Wilkes and J. L. Williams, *J. Phys. Chem.*, 1984, **88**, 2614–2621.
51 R. L. Gardas and J. A. P. Coutinho, *AIChE J.*, 2009, **55**, 1274–1290.

